

Two-dimensional Bose-Einstein condensates in a CO₂-laser optical lattice

Giovanni Cennini^{1,*}, Carsten Geckeler^{1,**}, Gunnar Ritt^{1,2}, Tobias Salger¹, and
Martin Weitz^{1,2,***}

¹ Physikalisches Institut der Universität Tübingen, Auf der Morgenstelle 14, 72076 Tübingen, Germany

² Institut für Angewandte Physik der Universität Bonn, Wegelerstraße 8, 53115 Bonn, Germany

Published online 4 August 2006

PACS 03.75.Lm, 32.80.Pj, 05.40.Fb

We report on experiments with all-optically produced Bose-Einstein condensates in a mesoscopic optical lattice. By retroreflecting the radiation of a CO₂-laser operating near 10.6 μm, a lattice with spacing between sites of $\lambda_{\text{CO}_2}/2 \simeq 5.3 \mu\text{m}$ is realized, for which atom tunneling is negligible. Once cooled to quantum degeneracy by direct evaporative cooling in the lattice, the properties of the trapped microclouds can be studied with far field interference experiments. The microscopic atom clouds are shown to be in the two-dimensional regime for small atom filling. The realized system has extremely long coherence times, and holds fascinating prospects for both quantum logic and the study of novel collective phenomena.

© 2006 WILEY-VCH Verlag GmbH & Co. KGaA, Weinheim

1 Introduction

Cold atoms in optical lattices provide a very clean testing ground for effects known from solid state physics, such as Bloch oscillations or the Mott-insulator phase transition [1]. In these experiments, “conventional” lattices were used where the spacing between sites is close to half the wavelength of the lowest absorption lines, yielding spacings below half a micron for alkali atoms. For typical parameters of quantum gas experiments, the tunneling time between sites is much lower or comparable with the available coherence times. Much less investigated are lattices with truly independent sites, where the tunneling between sites is negligible. As a loading of quantum degenerate atoms into extremely deep lattices is difficult, this usually requires a spacing between sites clearly above the trapping wavelength. In our experiment, such a lattice is realized by retroreflecting the radiation near a wavelength of 10.6 μm provided by a single-frequency CO₂-laser, yielding a spacing between sites of 5.3 μm [2]. Other techniques rely on holographic methods [3], the inclination of two closer resonant laser beams under a small angle [4] or optical microstructures [5]. A few of those techniques have also been used with quantum degenerate atomic samples [2, 4]. Interestingly, in anisotropic traps the physics can become one- or two dimensional [6–9]. Optical lattices provide an ideal testing ground for the study of the physics in reduced dimensions. Lattices with negligible coupling between sites also hold fascinating prospects for quantum computing with neutral atoms [10–12] or the generation of arrays of atom lasers [13].

We here describe an experiment realizing an array of disk-shaped $m_F = 0$ microcondensates in the antinodes of a standing wave near 10.6 μm. The atoms are directly cooled to quantum degeneracy in the independent sites of the mesoscopic lattice. We have studied the far field interference pattern of the independent coherent atom sources. The observed interference contrast decreases with the number of sources.

* Present address: Philips Research, 5656AE Eindhoven, The Netherlands

** Corresponding author E-mail: geckeler@pit.physik.uni-tuebingen.de

*** E-mail: martin.weitz@uni-bonn.de

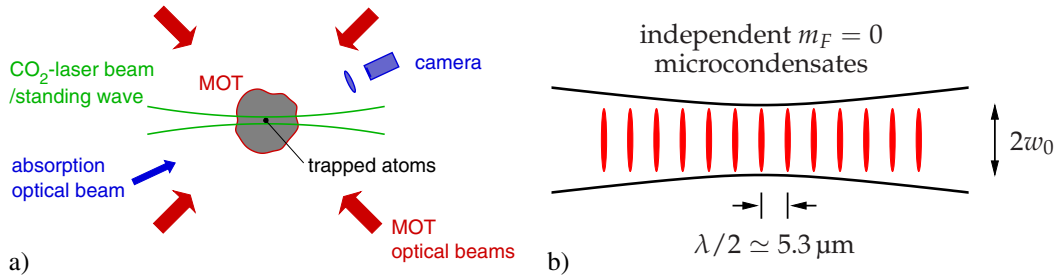


Fig. 1 a) Schematic setup of the experiment. b) Geometry of the mesoscopic optical lattice.

Our results well agree with a random-walk model, predicting a $1/\sqrt{N}$ scaling of the fringe contrast with the condensate number N . The time-of-flight images of the expanded array also allows us to study the dimensionality of the trapped atom clouds. The results indicate that the axial dimension is frozen out, so that the trapped microclouds are in the two-dimensional regime.

2 Experimental setup and procedure

A scheme of our experimental setup along with the geometry of the one-dimensional mesoscopic lattice is shown in Fig. 1. For a more detailed description of the apparatus, see [2, 14]. Our experiment starts with the trapping and cooling of bosonic atoms in a magneto-optical trap (MOT). Atoms of the isotope ⁸⁷Rb are collected and pre-cooled in a magneto-optical trap (MOT), which is loaded from the thermal gas emitted by heated rubidium dispensers placed inside the vacuum chamber. The light for the MOT is generated by two grating stabilized diode lasers.

The optical dipole trap is realized by tightly focussing a CO₂-laser beam whose wavelength is near 10.6 μm. This mid-infrared light passes an acousto-optic modulator (AOM) which provides optical isolation and allows for a control of the beam intensity. The transmitted beam enters a vacuum chamber and is focused by an adjustable ZnSe lens placed inside the vacuum chamber. By means of a further lens and an external retroreflecting mirror an intense one dimensional standing wave is formed. The longitudinal axis of this mid-infrared standing wave is orthogonal to the gravity axis. The size of the beam waist in the trapping region can be varied with an external telescope within a range of 20–40 μm. This gives us control over the number of populated trapping sites, and on the relative strength of the trap frequencies.

Throughout the MOT loading stage, the CO₂-laser beam is kept on at full power (30 W). In order to enhance the atom transfer from the MOT into the purely optical dipole trap, a transient compression of the atomic cloud is achieved with a dark-MOT phase which lasts about 60 ms. During this period, the MOT cooling laser is detuned to the red of the cooling transition by 180 MHz, and the repumping laser intensity is decreased by roughly a factor 100. In this way, atoms are pumped into the lower hyperfine state, reducing light assisted losses and allowing for higher densities, thus improving the overlap between the MOT and the dipole potential.

The CO₂-laser dipole trapping geometry results in an array of disk-shaped microtraps. If we assume that this beam travels along the z direction and that is perpendicular to the gravity direction x , the analytical form of the external potential can be expressed as:

$$U(x, y, z) = \frac{2\alpha_s P}{\pi c \epsilon_0 w_0^2 s(z)^2} e^{-\frac{2(x^2+y^2)}{w_0^2 s(z)^2}} [1 + \cos(2kz)] - mgx \quad (1)$$

where $s(z) = \sqrt{1 + (z/z_0)^2}$, $z_0 = \pi w_0^2/\lambda$, m is the mass of the atoms and g the acceleration due to gravity. In this formula, the beam waist of the laser beam is w_0 ($1/e^2$ radius) and the optical power is P .

We note that adjacent sites are spaced by $d = \lambda_{\text{CO}_2}/2 \simeq 5.3 \mu\text{m}$, which is sufficiently far apart that tunneling between sites is completely negligible. The aspect ratio of these microtraps is characterized by the vibrational frequencies $\nu_r/\nu_z = \sqrt{2}\lambda/2\pi w_0$. For typical lattice experiments, the beam waist w_0 was chosen to be $37 \mu\text{m}$. When a perfect alignment is realized, each microtrap has an aspect ratio of nearly 15. Because of the relatively tight longitudinal confinement along the lattice z axis, the atomic motion along this axis is frozen out and atoms only move in the orthogonal x, y plane.

Once the atoms are trapped in the antinodes of the CO_2 -laser optical lattice, we apply forced evaporation directly in the dipole potential in order to achieve quantum degeneracy [14–18]. For an efficient evaporation of hot atoms, we initially use a running wave geometry by misadjusting the CO_2 -laser beam backreflection mirror away from a perfect retroreflection. This is achieved by tilting this mirror with the help of an electronically driven piezo. Rubidium atoms from a magneto-optical trap (MOT) are loaded into the running wave geometry. After this transfer, some 10^6 atoms, populating the lower hyperfine ground state ($F = 1$, $m_F = 0, \pm 1$) are left in the optical trap at a temperature near $100 \mu\text{K}$. To cool the trapped atomic cloud, the CO_2 -laser beam power is acousto-optically ramped down to induce forced evaporative cooling. The total evaporation stage lasts about 10 seconds, during which the mid-infrared beam power is smoothly reduced from 30 W to a typical final value of 40–50 mW. Throughout the evaporation stage, the MOT quadrupole field with 10 G/cm field gradient is left on. This gradient is sufficiently strong to remove atoms in field-sensitive spin projections in this running wave geometry [14]. While the initial phase of this evaporation is performed in the running wave geometry, cooling to quantum degeneracy is achieved in the lattice geometry. By the end of the evaporative cooling stage, we thus slowly switch to a standing wave geometry by servoing the piezo-mounted mirror correspondingly. The 1D optical lattice geometry is fully aligned at a time of 1–2 seconds before the onset of quantum degeneracy (corresponding to an atomic temperature of a factor 2 above the BEC transition temperature). This ensures that the microcondensates are formed independently. At the end of the evaporation state, an array of $m_F = 0$ microcondensates is created. The total number of atoms in the optical lattice is about 7000, and the number of condensed lattice sites can be varied from typically 5 to 35 by choosing different beam waists of the lattice beams and — in a smaller range — also by allowing for small misalignments of the lattice beams. For all our measurements, the estimated tunneling time between sites is longer than the age of the universe. The residual sensitivity of the $m_F = 0$ condensates to stray magnetic fields due to the second order Zeeman shift is near 14 fK/mG^2 . For a typical spatial extension of the lattice of $100 \mu\text{m}$, the variation of the condensate phases due to magnetic field inhomogeneities is 0.15 Hz at an estimated field gradient of 50 mG/cm .

3 Experimental results

For an analysis of the array of microcondensates, we have studied absorption images observed after releasing the atoms (see Figs. 2a,b). A few ms after extinguishing the confining lattice potential, the clouds spatially overlap, and an interference pattern of the independent clouds can be observed, as shown in the second image recorded after 15 ms free expansion time. A horizontal profile of this image is shown in Fig. 2c. Our experimental imaging resolution only allows us to resolve the fringe pattern arising from the interference of adjacent sites. Notably, the contrast and the phase of the fringe pattern is different for each realization of the experiment. Fig. 3a in a polar plot shows the fitted fringe contrast and phase for 130 different measurements. It can be clearly seen that the phase (i. e. position of the fringe pattern) varies from run to run. This can be understood in terms that each of the independently created condensates, despite being initially in a state with undefined phase, upon measurement develops a well-defined relative phase that is random in each of the realizations [19–21]. The expected fringe contrast for an array of N coherent sources can very elegantly be calculated with a random-walk model in which the number of steps equals the number independent phases, i. e. $N - 1$ [22]. The calculations predict a $1/\sqrt{N}$ scaling of the average visibility with the condensate number N . This reduction of fringe contrast with the number of sources can intuitively be understood as follows. When two independent condensates with equal number of atoms interfere, the

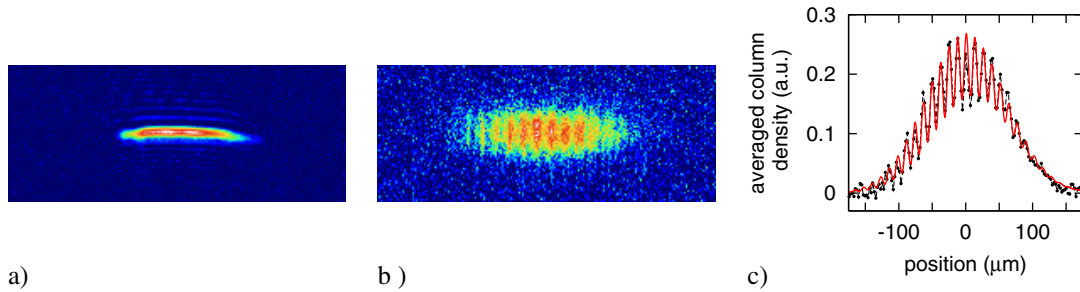


Fig. 2 a) False-color absorption image of 20 microcondensates recorded shortly after switching off the CO₂-laser trapping potential. b) False-color absorption image of an interference pattern of 20 independently generated $m_F = 0$ microcondensates released from a CO₂-laser optical lattice. This image was recorded after a free expansion time of 15 ms. The field of view is $350 \mu\text{m} \times 140 \mu\text{m}$. c) Horizontal profile of image b) averaged over a vertical region of $35 \mu\text{m}$: Experimental data (dashed line with dots) and fitted fringe pattern (solid line).

relative phase varies from run to run, but in all cases a density modulation with 100 % fringe contrast is expected. In the case of three interfering condensates two relative phases come into play. We in general expect that the phase difference between any two of the condensates differs from that between either one of them and the third one. One still expects a fringe pattern, but in general with reduced contrast. For a still larger number of sources, the degree of randomness increases. Interference patterns of condensates released from periodic lattice potentials are commonly investigated [1], but the interference of a larger number of independent condensates was not studied until Hadzibabic et al. [4] recently observed the interference from 30 independent condensates regularly spaced in a one-dimensional lattice and obtained the surprisingly high average fringe contrast of 34 %, which was indeed comparable to the results observed in the early two-condensates interference experiments of [23].

We have experimentally studied the dependence of the interference contrast on the number of condensates [2]. The corresponding results are shown in Fig. 3b. The observed average interference contrast decreases with source number N and agrees well with the result of a theoretical model based on a random walk of the probability amplitude in the complex plane. While the exact result can be given in terms of Klyver's formula, for a large number of condensates a $1/\sqrt{N}$ scaling of the average fringe contrast is obtained, as given by the central limit theorem [24]. When taking into account the reduction of the contrast due to our experimental imaging resolution, our results agree well with the theoretical predictions.

In subsequent experiments, we have verified whether the produced Bose-Einstein microcondensates are in the two-dimensional regime. For these measurements, the atomic expansion velocity after extinguishing the trapping potential was analyzed for different number of atoms in the condensates. In Figs. 2a,b, typical absorption images of the array of microcondensates before and after free expansion had been shown. From such images of the released array, we have derived the corresponding lengths of the expanded clouds along the longitudinal and the radial axis respectively. Figs. 4a and b now show the condensate's expansion during 15 ms of free flight along both directions for different atom numbers. Because the atomic oscillation frequency in the longitudinal direction is much higher than that in the radial plane, one intuitively would expect that the expansion in the longitudinal axis is much faster than that in the radial plane. Experimentally, the measured expansions along both directions however are quite comparable. This is attributed to the issue that the trapped atom clouds are in the two-dimensional regime, i. e. the longitudinal (z -) axis is frozen out. As a further evidence for the reduced dimensionality, one notices that the observed expansion along the z -axis is more or less independent on the number of atoms (note that even a small decrease with the number of atoms seems to be present). In contrast, the expansion along the radial axis clearly increases with the number of atoms in the microclouds. This again is an indication for the axial direction being frozen out, with the spatial expansion here being determined only by the momentum uncertainty of the harmonic oscillator ground state, i. e. independent of atom density dependent mean field effects.

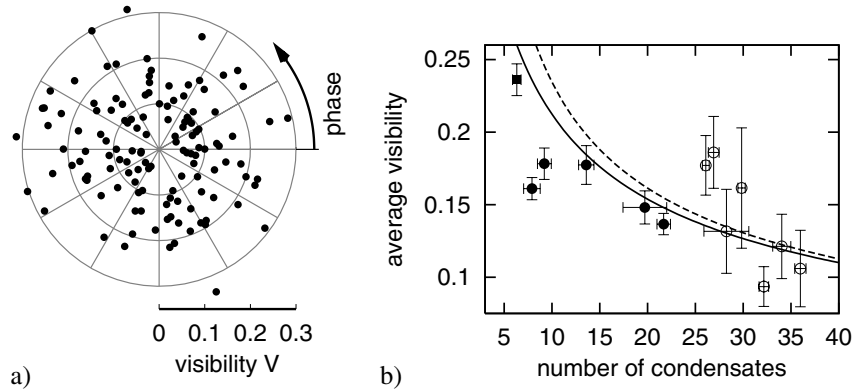


Fig. 3 a) Visibilities and phase angles of fringe patterns arising from the interference of 20 independent Bose-Einstein condensates, as derived from fits as in Fig. 2c, have been drawn (dots) in a polar diagram for 130 different realizations of the experiment. b) Average fringe visibilities of far field interference patterns as a function of number of interfering coherent atomic sources. The experimental data sets were recorded with beam waists: $24.3 \mu\text{m}$ (squares), $30.0 \mu\text{m}$ (dots), and $40.2 \mu\text{m}$ (circles). The data has been fitted with the theoretical calculated fringe contrast multiplied by a constant factor, which is left as a free parameter to account for the finite imaging resolution (solid line). The dashed line gives the corresponding result in the central limit approximation when assuming the same imaging resolution.

The truly two-dimensional regime is expected to occur if both the chemical potential μ of each microcondensate and $k_{\text{B}}T$, where T denotes the atomic temperature, are much smaller than the harmonic oscillator energy along z direction, namely $\hbar\omega_z$ [8]. The measured number of atoms in each microcondensate in our experiment is in the range between 100 and 400. For a typical value of the CO_2 -laser beam waist of $37 \mu\text{m}$ the vibrational frequencies at the end of the evaporation process were measured to be $\omega_z = 2\pi \times 2160 \text{ Hz}$ and $\omega_r = 2\pi \times 150 \text{ Hz}$. Given these parameters, one can derive the maximum allowed number of atoms in each site N_s of the optical lattice for which the condition $\mu \ll \hbar\omega_z$ is still fulfilled. One obtains the condition

$$N_s \ll N_{\text{max}} = \sqrt{\frac{32\hbar}{225ma^2}} \sqrt{\frac{\omega_z^3}{\omega_r^4}} \quad (2)$$

In our experiment, we estimate N_{max} to be $\simeq 3400$. Because the atom number in each site is only a few hundreds, we anticipate that the condition $\mu \ll \hbar\omega_z$ is clearly fulfilled in our lattice.

The second condition for the atoms to be in the fully two-dimensional regime is that $T \ll \hbar\omega_z/k_{\text{B}} \simeq 104 \text{ nK}$. As no thermal cloud could be detected in the described experiments, we assume that the atomic temperature is clearly below the BEC transition temperature, i.e. $T \ll T_c$. The transition temperature can be calculated from the measured vibrational frequencies and the number of atoms per site N_s to be $T_c = 0.94 \hbar(\omega_r^2\omega_z)^{1/3}/k_{\text{B}} \cdot N_s^{1/3} \simeq 16 \text{ nK} \cdot N_s^{1/3} \simeq 96 \text{ nK}$ for $N_s = 200$. That is to say that for small atom numbers and $T \ll T_c$ the condition $T \ll \hbar\omega_z/k_{\text{B}}$ is also fulfilled. We conclude that the two-dimensional regime is fully reached in the mesoscopic lattice for the used parameters.

An interesting question is whether phase fluctuations, which are generally more severe in low-dimensional condensates, significantly reduce the coherence of the microcondensates. In a recent interference experiment with a small number of two-dimensional condensates, phase defects were monitored at temperatures slightly below the BEC transition temperature [9]. For the parameters used in our experiments, no signatures for such defects could be observed from the fringe pattern.

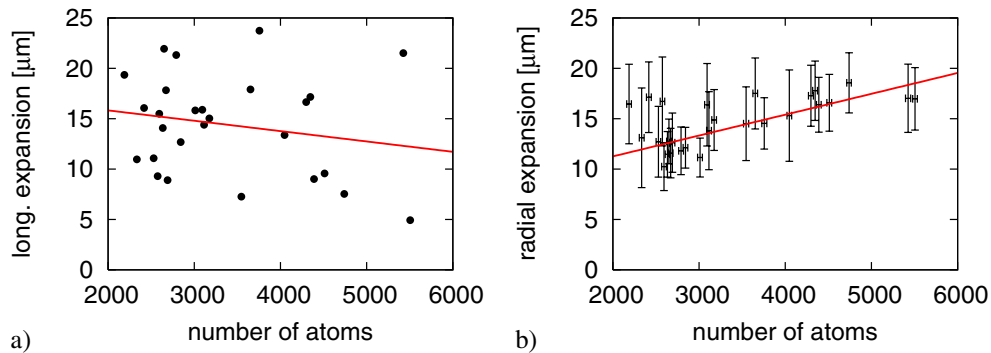


Fig. 4 Measured spatial expansion of the microcondensates in the mesoscopic optical lattice in the longitudinal and radial direction after a free drift time of 15 ms as a function of the number of atoms in all lattice sites.

4 Conclusions

To conclude, we have generated an array of Bose-Einstein condensates in a mesoscopic optical lattice. The condensates are formed by atoms in the $m_F = 0$ spin-projection, with their chemical potential being first-order insensitive to magnetic stray fields. The observed average interference visibility decreases with the condensate number. An analysis of the expansion of the array of microcondensates shows that the microclouds are in the two-dimensional regime. Notably, the lower dimensional regime is entered during the condensation process itself. The experiments here reported give a very direct way for the production of an array of quantum degenerate gases in lower dimensions.

For the future, it is anticipated that mesoscopic optical lattices hold fascinating prospects for the observation of new quantum phases. The described system is e. g. of interest for the study of collective quantum states in rapidly rotation traps, as multiparticle states with anyonic statistics of quasiparticles [25]. A different perspective is the possible observation of correlated insulator phases [1], such as the Mott transition, in a system which allows for an optical resolving of individual lattice sites [26]. For extremely low values of the lattice depth, a tunneling between sites can be achieved despite the large lattice spacing, as has been recently demonstrated for a double-well potential [27]. For such weakly confined systems, long scattering lengths are very useful, as can be very elegantly reached with Feshbach tuning in fermionic atoms [28]. The in this way produced strongly interacting periodic systems can have prospects for the observation of solid state effects in the spatial domain. Along different lines, such systems with individual lattice sites being optically addressable, hold fascinating prospects for quantum computing in optical lattices [10, 11, 29].

Acknowledgements We acknowledge financial support from the Deutsche Forschungsgemeinschaft, the Landesstiftung Baden-Württemberg, and the European Community.

References

- [1] See e. g., I. Bloch, *Phys. World* **17**, 25 (2004).
- [2] G. Cennini, C. Geckeler, G. Ritt, and M. Weitz, *Phys. Rev. A* **72**, 051601(R) (2005).
- [3] D. Boiron et al., *Phys. Rev. A* **57**, R4106 (1998).
- [4] Z. Hadzibabic et al., *Phys. Rev. Lett.* **93**, 180403 (2004).
- [5] R. Dumke et al., *Phys. Rev. Lett.* **89**, 097903 (2002).
- [6] F. Schreck et al., *Phys. Rev. Lett.* **87**, 080403 (2001).
- [7] A. Görlitz et al., *Phys. Rev. Lett.* **87**, 130402 (2001).
- [8] T. Stöferle, H. Moritz, C. Schori, M. Köhl, and T. Esslinger, *Phys. Rev. Lett.* **92**, 130403 (2004); M. Köhl, H. Moritz, T. Stöferle, C. Schori, and T. Esslinger, cond-mat/0404338.

- [9] S. Stock, Z. Hadzibabic, B. Battelier, M. Cheneau, and J. Dalibard, *Phys. Rev. Lett.* **95**, 190403 (2005).
- [10] G. Brennen, C. Caves, P. Jessen, and I. Deutsch, *Phys. Rev. Lett.* **83**, 1060 (1999).
- [11] D. Jaksch, H.-J. Briegel, J. I. Cirac, C. W. Gardiner, and P. Zoller, *Phys. Rev. Lett.* **82**, 1975 (1999).
- [12] O. Mandel et al., *Nature* **425**, 937 (2003).
- [13] G. Cennini, C. Geckeler, G. Ritt, and M. Weitz, *cond-mat/0510629*.
- [14] G. Cennini, G. Ritt, C. Geckeler, and M. Weitz, *Phys. Rev. Lett.* **91**, 240408 (2003).
- [15] M. Barrett, J. Sauer, and M. S. Chapman, *Phys. Rev. Lett.* **87**, 010404 (2001).
- [16] T. Weber et al., *Science* **299**, 232 (2003).
- [17] S. R. Granade, M. E. Gehm, K. M. O'Hara, and J. E. Thomas, *Phys. Rev. Lett.* **88**, 120405 (2002).
- [18] Y. Takasu et al., *Phys. Rev. Lett.* **91**, 040404 (2003).
- [19] J. Javanainen and S. M. Yoo, *Phys. Rev. Lett.* **76**, 161 (1996).
- [20] M. Naraschewski et al., *Phys. Rev. A* **54**, 2185 (1996).
- [21] Y. Castin and J. Dalibard, *Phys. Rev. A* **55**, 4330 (1997).
- [22] S. Ashhab, *Phys. Rev. A* **71**, 063602 (2005).
- [23] M. R. Andrews et al., *Science* **275**, 637 (1997).
- [24] See e. g.: E. Merzbacher, J. M. Feagi, and T.-H. Wu, *Am. J. Phys.* **45**, 964 (1977).
- [25] N. K. Wilkin, and J. M. F. Gunn, *Phys. Rev. Lett.* **84**, 6 (2000); B. Paredes, P. Fedichev, J. I. Cirac, and P. Zoller, *Phys. Rev. Lett.* **87**, 010402 (2001).
- [26] R. Scheunemann, F. S. Cataliotti, T. W. Hänsch, and M. Weitz, *Phys. Rev. A* **62**, 051801 (R) (2000).
- [27] M. Albiez et al., *Phys. Rev. Lett.* **95**, 010402 (2005).
- [28] D. S. Petrov, C. Salomon, and G. V. Shlyapnikov, *Phys. Rev. Lett.* **93**, 090404 (2004).
- [29] S. Friebel, C. D'Andrea, J. Walz, M. Weitz, and T. W. Hänsch, *Phys. Rev. A* **57**, R20 (1998).